

# ADVANCED CONTROLS OF ORGANIC RANKINE CYCLE FOR HIGHLY TRANSIENT FLUCTUATIONS DURING INITIAL STARTUP

Parsa Mirmobin\*, Chris Sellers

Calnetix Technologies, LLC  
16323 Shoemaker Ave, Cerritos, CA 90703  
USA  
e-mail: pmirmobin@calnetix.com, csellers@calnetix.com  
Web page: <http://www.calnetix.com>

\* Corresponding Author

## ABSTRACT

Organic Rankine Cycles are typically utilized in systems with a steady heat source and condensing condition. In highly transient cases, the working fluid undergoes violent phase transition within the evaporator. The resulting forces are experienced by the heat exchanger, expander, and associated piping. This ultimately results in premature and catastrophic component failure.

This paper discusses pressure and flow instability which occurs during initial startup of an ORC. The instability is a result of the interaction between the nonlinear pressure field within the evaporator and the pressure source (centrifugal pump.) The phenomenon is characterized by a rapid oscillation in pressure and flow and resembles similar effects observed in low pressure boilers and axial compressors. Experimental data is examined and a method for reducing or eliminating this effect is presented.

## 1. INTRODUCTION

Organic Ranking Cycles (ORC) may experience large oscillations in evaporator outlet pressure, mass flow, and temperature during initial startup. These oscillations cause unstable operation, premature shutdown, and increased component wear. When designing an overall control scheme, it is important to account for this phenomenon to ensure a safe and stable startup.

Two-phase flow instabilities were first studied by Ledinegg (1938). He observed the internal characteristic curve (system curve) for an evaporator has a region of negative slope region caused by the phase change from liquid to vapor. Figure 1 below is a graphical representation of the negative sloped curve.

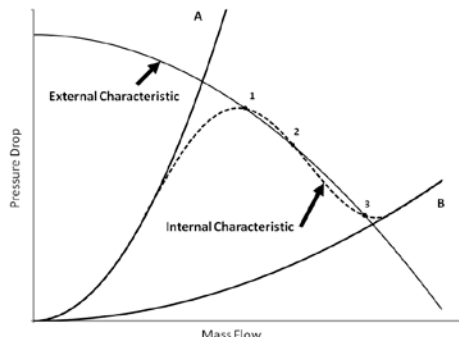


**Figure 1:** Negative Slope of Internal Characteristic Curve

Curve A represents the internal characteristic of an evaporator filled primarily with vapor. Curve B represents the internal characteristic of an evaporator filled primarily with liquid. As the pressure and mass flow increase, the evaporator's internal characteristic transitions between curves A and B along the dotted line. In Figure 1 the external characteristic (pump curve) intersects the evaporator's internal characteristic at points 1, 2, and 3. Points 1, 2, and 3 each represent stable operating conditions for the pump. A small perturbation in the mass flow or pressure drop will cause the pump to jump from one point to the other. Thus this operating condition is unstable.



**Figure 2:** Model to Describe Density Wave Oscillations

Subsequent studies focused on dynamic instabilities with a repeating oscillatory pattern. The most common type of dynamic instability is the density wave oscillation, DWO, first discussed by Stenning (1964). Figure 2 shows the classical model used to describe DWO. It consists of a pipe with throttling valves upstream and downstream of a heated section. The pressure at the pipe inlet and exit are constant at  $P_i$  and  $P_e$ . At some time "t" the pressure at  $P_2$  undergoes a small drop of the order  $\Delta P$ . This pressure drop may be caused by unsteady flow conditions, fluctuations in the two-phase region, etc. The pressure at  $P_1$  drops nearly instantly by an equal value of  $\Delta P$ . The pressure difference between  $P_i$  and  $P_1$  increases and thus the fluid velocity into the heated section increases by:

$$u \propto \sqrt{P_i - P_1} \quad (1)$$

This sends a surge of higher density fluid through the heated section from  $P_1$  to  $P_2$ . The high density fluid causes an increase of the pressure of  $P_2$  by a value  $\Delta P$ . The pressure at  $P_1$  sees an equal increase and corresponding drop in the inlet velocity by Equation (1). Now a low density surge of fluid is sent from  $P_1$  to  $P_2$ , and the cycle repeats itself.

Flow stall and reversal plays a major role in the flow instabilities present during an ORC system's startup. A parallel may be drawn with compressor surge oscillations. Axial compressors exhibit a sharp drop in the head output at very low flows. Surge oscillations occur when an axial compressor operates with high throttling and a large compressible volume in the downstream plenum. The oscillation cycle is described as:

1. Pressure builds downstream in the plenum.
2. Compressor flow decreases and pressure output increases following the compressors external characteristic curve.
3. The pressure output reaches a peak value after which flow separation occurs on the compressor blade surface. This causes the compressor head output to drop dramatically.
4. Pressure in the plenum decreases and flow reversal may occur due to the breakdown of the flow field within the compressor.
5. Once the plenum pressure is sufficiently low, the flow within the compressor stabilizes. Flow begins to move forward into the plenum and the pressure begins to rise again.

The interested reader is referred to Moore and Greitzer (1986) for a more detailed description.

In the next section experimental results will be presented, and attempt will be made to provide a qualitative description of the oscillation process which occurs during the startup of an ORC system.

## 2. EXPERIMENTAL RESULTS

### 2.1 Methodology

Data was collected using the Calnetix ORC test cell partially depicted in Figure 3. The working fluid was R245fa refrigerant. A Calnetix ORC system was operated with the turbine in bypass. A

throttling valve was used to represent the pressure drop action of the turbine. Heat was added to the system via a PID controlled hot water loop. The hot water loop was operated at two heating condition: 21 kg/s at 71°C and 28 kg/s at 82°C. The working fluid pump was stepped from 6Hz to 35Hz in 1Hz increments over a period of 75 minutes. The stepping procedure was stopped at various frequencies in order to allow transient phenomena to decay and capture the sustained oscillatory phenomena. Table 1 provides a description of each sensor in the test apparatus. Data was acquired with a sampling frequency of 5Hz for TT106, FM101, TT111, PT112, and PT113 and with a sampling frequency of 0.333 Hz for TT20 and PT20. The initial condition for these sensors prior to pump operation are listed in Table 1.

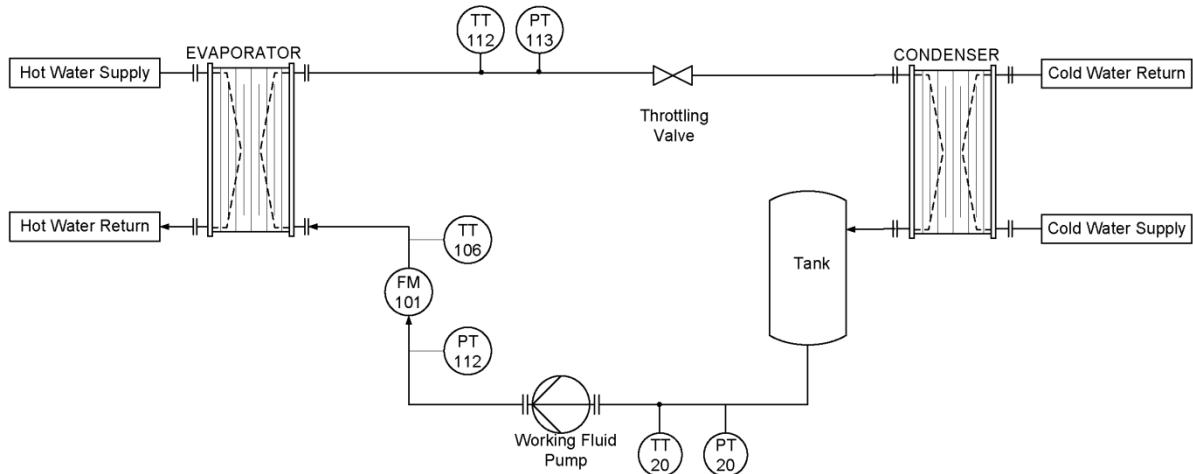


**Figure 3:** Test Apparatus

**Table 1:** Test Apparatus Sensor Descriptions

Sensor Tag	Description
TT20	Working fluid Tank Temperature
PT20	Working fluid Tank Pressure
TT106	Evaporator Inlet Temperature
PT112	Evaporator Inlet Pressure
TT112	Evaporator Outlet Temperature
PT113	Evaporator Outlet Pressure
FM101	Working fluid Mass Flow Meter

**Table 2:** Sensor Initial Conditions

Sensor Tag	Initial Values
TT20	19.7 °C
PT20	1.4 Bar
TT106	25.6 °C
PT112	1.3 Bar
TT112	61.6 °C
PT113	2.3 Bar
FM101	0.2 kg/s

## 2.2 Results and Discussion

Figure 4 shows a representative diagram of the oscillatory process.

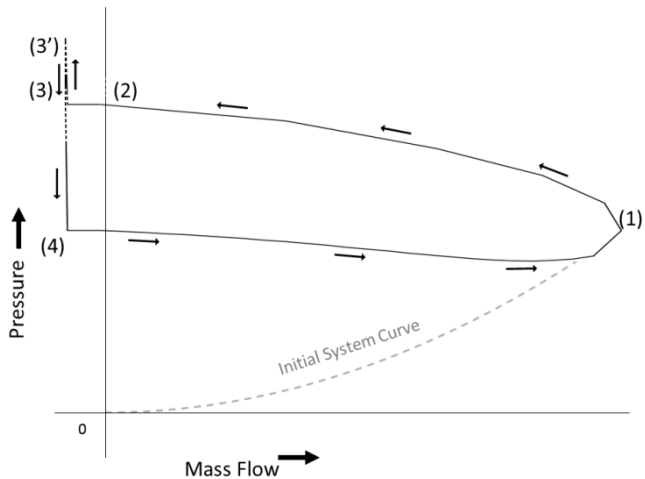


**Figure 4:** Diagram of Pressure/Mass Flow Oscillations

Initially the evaporator is completely filled with vapor. The pump is operated to some driving frequency and high density liquid flows into the evaporator. The pressure in the evaporator rises to point 1 following a path similar to Curve A in Figure 1. The liquid quickly vaporizes and an imbalance forms between vapor production and mass flow out of the evaporator. The accumulation of mass within the evaporator and increasing system enthalpy causes a local rise in pressure. The mass flow begins to slow down as the evaporator pressure rises, and the system transitions from operating point 1 to 2 along the pump's external characteristic curve. Flow stall and partial reversal occurs from points 2 to 3. At low pump frequencies, the evaporator pressure continues to build up to point 3' as the remaining liquid is vaporized. From point 3 (or 3') to point 4 the evaporator pressure drops as the gas expands forward through the throttling valve and backwards into the piping section between the pump and evaporator. Once the evaporator pressure reaches the original conditions at point 1, the pump is able to reestablish forward flow and the diagram transitions from point 4 to 1. The pump is again operating at point 1 and the cycle repeats.

It is believed flow reversal occurs due to flow separation along the impeller blade surfaces. The measured value for flow reversal was 0.18kg/s. At low frequencies, test data indicated gas was present in the pipe section between the pump and evaporator inlet. This would only occur if gas flows backwards from the evaporator. Additionally the temperature at the bottom of the working fluid tank shows a rapid spike during the flow reversal period. This is believed to be caused by higher temperature fluid from within the pump pushed backwards to the sensor.

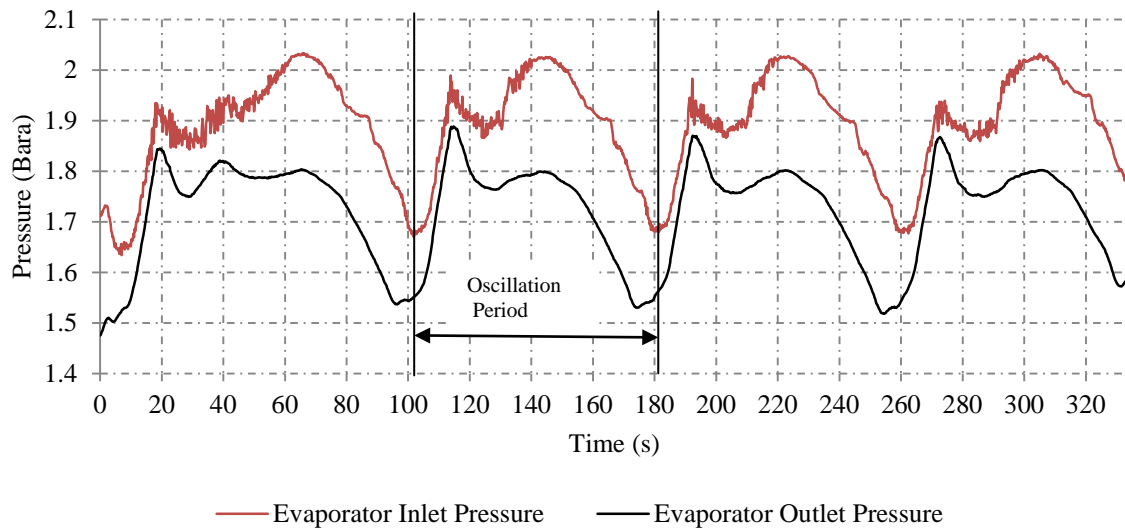


**Figure 5:** Low Frequency Pressure Oscillations at Pump Driving Frequency of 14 Hz

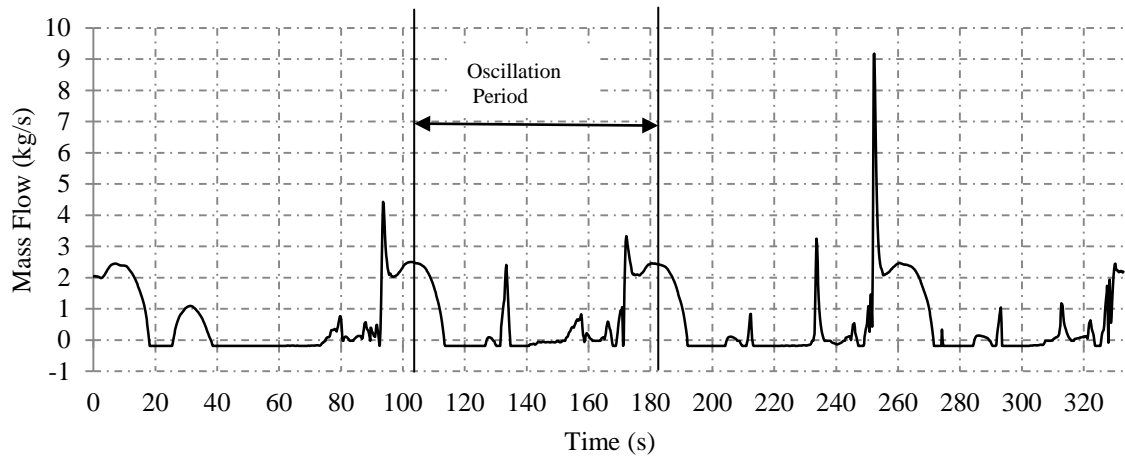


**Figure 6:** Low Frequency Mass Flow Oscillations at Pump Driving Frequency of 14 Hz

At low pump frequencies the pressure and mass flow oscillations resemble those depicted in Figure 5 and Figure 6. The oscillatory period ranges from 102 to 81 seconds. The period decreases with increasing pump frequency. The oscillations are characterized by a long flow stall and reversal period followed by a sudden surge in liquid flow. It is believed the lengthy flow stall/reversal period is caused by the residual liquid vaporizing within the evaporator. High frequency oscillations with periods shorter than the sampling frequency appear in the evaporator inlet pressure after the onset of flow reversal. These may be a product of pump cavitation induced by recirculating flow at the pump outlet.

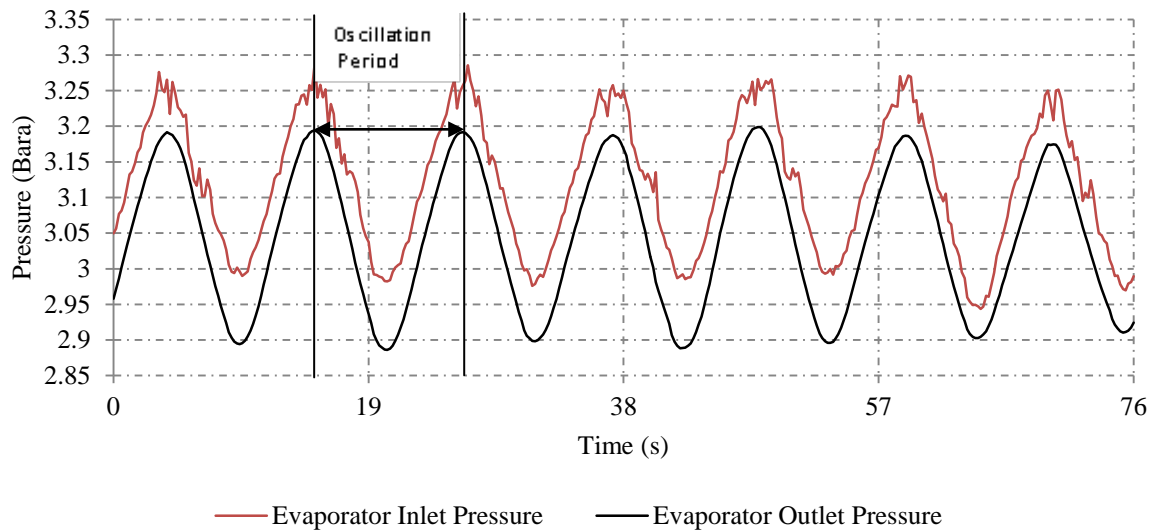


**Figure 7:** High Frequency Pressure Oscillations at Pump Driving Frequency of 25 Hz

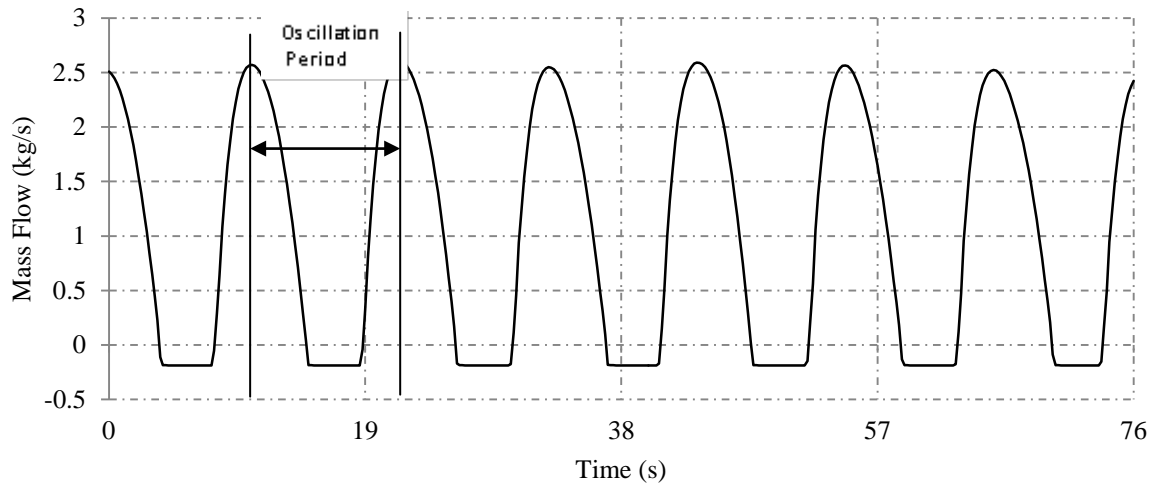


**Figure 8:** High Frequency Mass Flow Oscillations at Pump Driving Frequency of 25 Hz

As the pump driving frequency is increased further, a transition occurs from the low frequency pattern (Figure 5 and Figure 6) to a high frequency pattern shown in Figure 7 and Figure 8. The period of this high frequency oscillation ranged from 17 to 9 seconds. As before the oscillation period decreased with increasing pump driving frequency. These oscillations are characterized by a shorter mass flow stall/reversal period (~5 seconds vs ~70 seconds.) The shape of the pressure and mass flow oscillation is significantly more regular with a sinusoidal quality. Additionally the amplitude of the pressure and mass flow oscillations increased with increasing pump drive frequency.

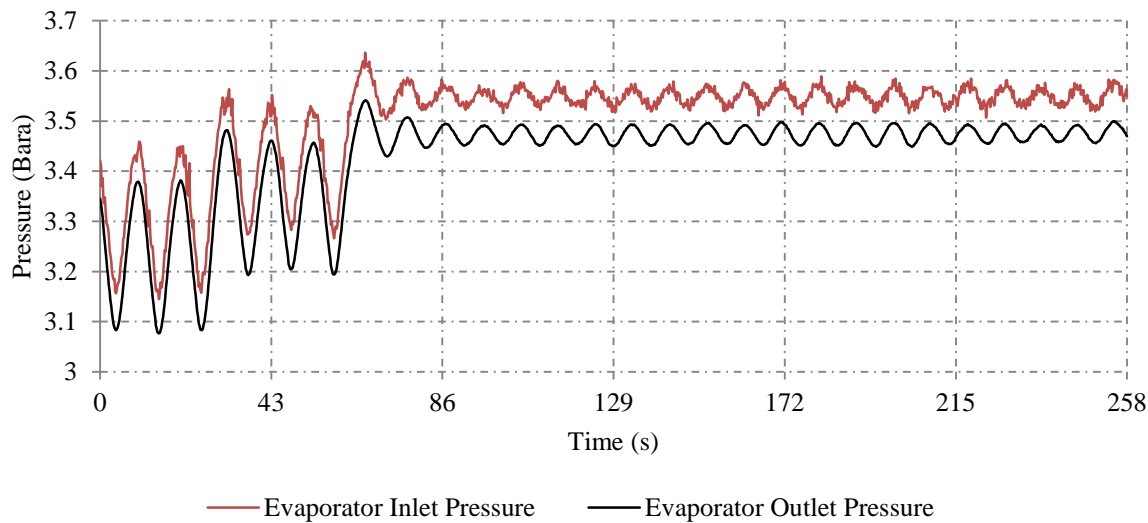


**Figure 9:** Pressure Oscillation Stabilization at Pump Driving Frequency of 27 Hz

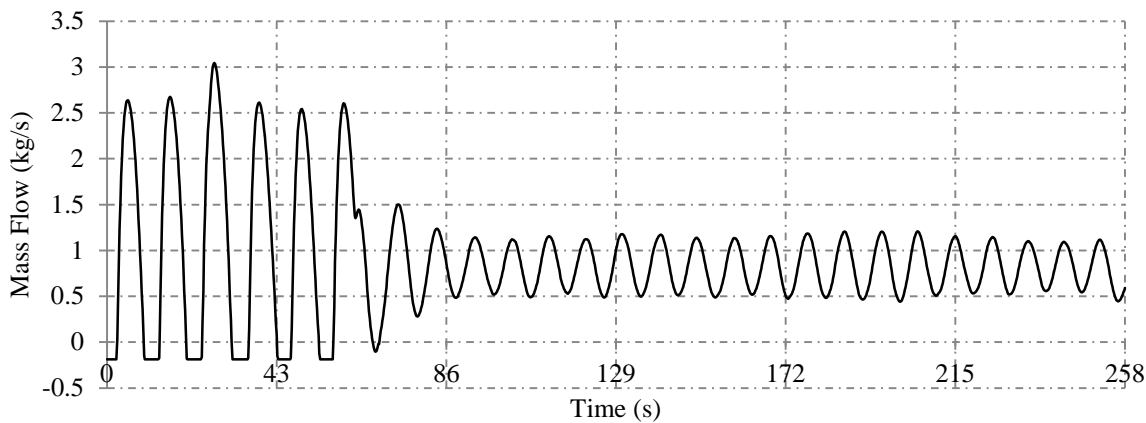


**Figure 10:** Flow Oscillation Stabilization at Pump Driving Frequency of 27 Hz

Figure 9 and Figure 10 show the pressure/mass flow oscillations stabilizing at high pump frequency. The flow stall/reversal pattern is no longer present. The large swings in flow and pressure stabilize to relatively smaller fluctuations. This stabilization may occur as the internal characteristic of the evaporator completes the transition from curve A to B in Figure 1, or it may be a result of the pump's external characteristic curve being sufficiently large to prevent flow stall/reversal.

The oscillatory patterns were very similar at the two source temperature and mass flow conditions. Increasing the source temperature and mass flow had the effect of increasing the stabilization frequency. Additionally the oscillation amplitude was greater for the higher temperature operation. It is believed this is due to increased pumping power at higher frequencies. This is in agreement with field observations which show the phenomena was more severe for higher temperature applications (e.g. those involving high temperature steam and exhaust gas.)

All the preceding data was collected for evaporator exit superheats on the order of 30°C. It was observed for superheat values less than ~10°C oscillations were not present. This may indicate a compressible volume is necessary for large amplitude oscillations to occur.

Based on the observations described above, it is believed evaporators with lower pressure loss (i.e. shell and tube) may be less prone to this type of instability. These types of evaporator are less commonly used in the field due to added cost of refrigerant charge and space limitations.

Additionally the use of a volumetric pump vs. a centrifugal pump may reduce or eliminate the oscillatory phenomena due to the steep external characteristic. In fact this type of pump is recommended in literature to avoid a Ledinegg type instability.

### 3. CONTROL AND DETECTION STRATEGIES

As seen in the previous section, the system stabilizes once the working fluid pump has reached a sufficiently large speed. Thus the simplest means to reduce pressure and flow oscillations is to ramp the pump speed quickly through the unstable operating conditions. Figure 11 shows the operation of a constant ramp pump signal and its primary control value, superheat.

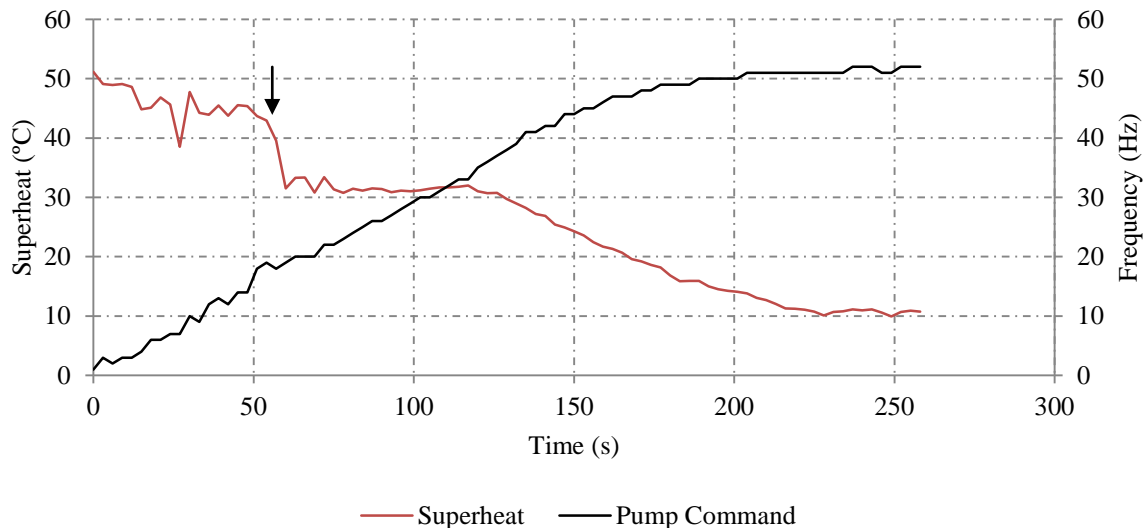


**Figure 11:** Fast Ramp through Unstable Region

There is a large drop in the superheat from approximately 45°C to 30°C at the 60 second mark (see arrow.) This is the result of a Ledinegg type flow excursion which occurs as the evaporator transitions from a primarily vapor to primarily liquid internal characteristic. During testing this excursion is accompanied by a "honking" noise and rush of fluid. The cause of this noise is not well understood. After the flow excursion, the superheat value is very stable and follows closely with the pump signal.

Detection of the onset of flow/pressure oscillations is accomplished by calculating the rate of change of the effected process value(s) as in Equation (2) below:

$$\frac{|X_n - X_{n-1}|}{\Delta t} \geq \alpha \quad (2)$$

where  $X$  is the process value of interest (e.g. superheat, pressure, or flow), the subscript "n" and "n-1" indicate the most recent sample and previous sample respectively,  $\Delta t$  is the sampling time, and  $\alpha$  is a threshold value. When the rate of change of the process value exceeds the threshold value, flow/pressure oscillations are present. From field testing a threshold valve may be derived which allows accurate detection of the oscillatory phenomena.

It should be noted, Equation (2) is prone to false detection due to signal noise. Noise filtering would require higher sampling frequency than the existing platform (PLC) allows. Inclusion of more historical terms in the equation will cause additional unacceptable delays due to slow sampling frequency. Therefore a more pragmatic approach has been devised to deal with the phenomena. After detection, the controller takes action to reduce the effects of the oscillatory phenomena. These actions

may result in an operating state which is not optimal for the desired system power output. Thereafter the system gradually migrates to the normal operating state. In this way even a false positive may be accommodated without causing the system to respond erratically or shutdown.

The control strategy present above has been successfully implemented in multiple field installations. Advanced control strategies require a more complete understanding of the underlying mechanism for the oscillatory phenomena and design factors which influence it (e.g. choice of evaporator, piping system design, etc.) This is the subject of future research projects.

#### **4. CONCLUSION**

In this paper an important source of instability in Organic Rankine Cycles is described, namely oscillatory pressure and mass flow within the evaporator. The underlying physical phenomena that lead to the oscillatory behavior have been discussed in detail. Experimental results show clear evident of the phenomena together with characteristics of such behavior. The paper goes on to outline the principles for detecting the oscillatory phenomena in operation. This sets the cornerstone for developing controls to mitigate or reduce this phenomena resulting in more stable and longer life operation.

#### **REFERENCES**

Ledinegg, M., 1938, "Instability of flow during natural and forced circulation", *Die Wärme*, Vol.61, No.8: P.891-898

Moore, F.K., Greitzer, E.M., 1986 "A Theory of Post-Stall Transients in Axial Compression Systems: Part I-Development of Equations, *J. Eng Gas Turbines Power*, 108: P.68-76

Hawkins, L., Zhu, L., Blumber, E., Mirmobin, P., and Erdlac Jr., R., 2012, Heat-To-Electricity with High-Speed Magnetic Bearing/Generator System, *GRC 2012 Annual Meeting*, Reno, NV.

Stenning, A.H., 1964, "Instabilities in the flow of a boiling liquid" *J. Basic Eng. Trans. ASME*, Ser. D.86: P.213-228